Diffusion-driven codimension-2 Turing-Hopf bifurcation in general Brusselator model

Lei Kong[1], Changrong Zhu[2]

[1]School of Mathematics and Statistics,

Guizhou University of Finance and Economics, Guizhou 550025, PR China

[2]College of Mathematics and Statistics,

Chongqing University, Chongqing 401331, PR China

Abstract

The spatiotemporal dynamics for general reaction-diffusion systems of Brusselator type under the homogeneous Neumann boundary condition is considered. It is shown that the reaction-diffusion system has a unique steady state solution. For some suitable ranges of the parameters, we prove that the steady state solution can be a codimension-2 Turing-Hopf point. To understand the spatiotemporal dynamics in the vicinity of the Turing-Hopf bifurcation point, we calculate and analyze the normal form on the center manifold by analytical methods. A wealth of complex spatiotemporal dynamics near the degenerate point are obtained. It is proved that the system undergoes a codimension-2 Turing-Hopf bifurcation. Moreover, several numerical simulations are carried out to illustrate the validity of our theoretical results.

Keywords: Turing-Hopf bifurcation; General Brusselator model; Normal form; Spatiotemporal dynamics; Center manifold

AMS(2010) Subject Classification: 37G05; 35K57; 92E20; 37G10

1 Introduction

The changes of dynamical structures for some system not only relate to time but also may depend on various independent variables such as location or age. Therefore, a diffusion process in the system can be improved by adding a spatial variable to the system. In fact, various diffusion phenomenon widely exist in physical, chemical, biological, environmental and sociological processes [12, 16, 42].

Since Turing published the seminal paper [46] in 1952, the spatiotemporal dynamics in reaction-diffusion system driven by linear diffusion has been widely studied [17, 24, 28, 48]. Turing suggested that diffusion could lead to instability and nonuniform spatial patterns. In other words, if a solution of the reaction system is stable, then the solution of the full reaction-diffusion system may be unstable. This is so-called Turing instability or diffusion-driven instability. Recently, many Turing-type models described by coupled systems of reaction-diffusion equations have been extensively studied in chemical and biological contexts [22, 27, 37, 40, 41].

In this paper, we shall consider the following general Brusselator model

$$\begin{cases} \frac{\partial u}{\partial t} - d_1 \triangle u = a - (1+b)u + f(u)v, & x \in \Omega,\ t > 0, \\ \frac{\partial v}{\partial t} - d_2 \triangle v = bu - f(u)v, & x \in \Omega,\ t > 0, \\ \frac{\partial u}{\partial n} = \frac{\partial v}{\partial n} = 0, & x \in \partial\Omega,\ t > 0, \\ u(x,0) = u_0(x) \geq 0, \quad v(x,0) = v_0(x) \geq 0, & x \in \Omega, \end{cases} \tag{1.1}$$

where $\Omega = (0, \ell\pi)$, $\triangle$ is the Laplace operator, ∂n is the outer flux, the unknown functions u, v represent the concentration of the two intermediary reactants having the diffusion rates $d_1, d_2 > 0$, positive constants $a, b > 0$ are the fixed concentrations, the initial values $u_0(x), v_0(x)$ are nonnegative continuous functions in $\bar{\Omega}$, and $f \in C^1(0,\infty) \bigcap C[0,\infty)$ is nonnegative and nondecreasing function. Many have extensively investigated various of Brusselator type in the last decades from both analytical and numerical viewpoint [2, 3, 15, 23, 35].

When $f(u) = u^2$, system (1.1) is a basic Brusselator model. The model was introduced by Prigogine and Lefever [34] in 1968, as a model for an autocatalytic oscillating chemical reaction [1, 43]. It consists of the following four intermediate reaction steps:

$$A \to X, \qquad B + X \to Y + D, \qquad 2X + Y \to 3X, \qquad X \to E.$$

The over-all reaction is $A + B \to D + E$ and it represent to the transformation of input products A and B into output products D and E. After some scalings and changes of variables, the four chemical reaction steps can be modeled by the mathematical model of system (1.1) with $f(u) = u^2$. Many mathematical properties of (1.1) with $f(u) = u^2$ have been exploited. Li et al. [26] carried out the Hopf bifurcation analysis, and the stability of the Hopf bifurcation periodic solution was discussed by applying the normal form theory and the center manifold theorem. The global bifurcation was discussed in [3]. The authors proved the existence of global continua for nontrivial solutions. Wit et al. [7] and Tzou et al. [8] studied the Turing stability of the positive steady state and derived the amplitude equations near the Turing-Hopf codimension-2 point. More results about the Brusselator system, one can see [9, 33, 35, 39, 49] and the references therein.

When $f(u) = u^p$ with $p > 0$, system (1.1) is a general Brusselator model. Without any restriction on the dimension of the domain, the upper and lower bounds for positive solutions, the existence and non-existence of positive steady states were obtained in [19]. Peng and Wang derived some results about the existence and non-existence of positive steady states by apply the implicit function theorem and topological degree argument in [36]. The existence of the Hopf bifurcation have been obtained by Guo et al. in [13]. And, the authors also got the positive steady state solutions and spatially inhomogeneous periodic solutions by numerical simulations.

When $f(u)$ is a nonnegative and nondecreasing functions, system (1.1) is a more general Brusselator model. Ghergu and Radulescu [18] revealed that the existence of Turing patterns strongly depends on the nonlinearity of f. More precisely, the authors pointed out that if f has a sublinear growth, then the system has no Turing patterns, while if f has a superlinear growth, then the existence of such patterns is related to the interdependence between the parameters a, b and d_1, d_2. The existence of Hopf bifurcation for the ordinary differential equation and partial differential equation models was obtained in [30], and by the center manifold theory and the normal form method, the bifurcation direction and stability of bifurcating periodic solutions were also established.

For system (1.1) with a nonnegative and nondecreasing function $f(u)$, the Turing instability or bifurcation analysis of codimension-1 such as Hopf bifurcation or steady state bifurcation were studied in [18, 30]. Note that the codimension-2 Turing-Hopf bifurcation can be viewed as the interactions of the codimension-1 Hopf and steady state bifurcations. Thence, the Turing-Hopf bifurcation may bring about mixed spatiotemporal

periodic patterns, domain structures displaying bi-stability between spatial and temporal modes, and spacetime chaos [20, 21, 29, 32, 50]. And, there is a lot of previous work on Turing-Hopf bifurcations of reaction-diffusion predator-prey systems by numerical method [4, 31, 38] or by analytical method [44, 45, 47].

In this paper, we will focus on the spatiotemporal dynamics near a codimension-2 Turing-Hopf bifurcation point of system (1.1). It is shown that system (1.1) has a steady state solution E^*. At E^*, system (1.1) has two conjugant imaginary eigenvalues with zero real part, and one zero eigenvalue. Others eigenvalues have nonzero real part. While from the eigenvalue theory, the so-called Turing-Hopf bifurcation occurs only if the theoretical eigenvalues of the spatially homogeneous system consist of one pair of purely imaginary eigenvalues together with a simple zero eigenvalue and the transverse condition holds. Through some computations, we will give out the transverse condition at which the codimension-2 Turing-Hopf bifurcation can occur. By calculating and analyzing the normal form on the center manifold, we will discuss the classification of the spatiotemporal dynamics in a neighborhood of the Turing-Hopf bifurcation point in detail.

The paper is organised as follows. In Section 2, we investigate the existence of Turing-Hopf bifurcation. The explicit computation of the normal form for Turing-Hopf bifurcation is presented in Section 3. The complex spatiotemporal dynamics near the Turing-Hopf bifurcation point of the system (1.1) are carried out by numerical simulations in Section 4. This paper ends with a brief conclusion in Section 5.

2 Existence of Turing-Hopf bifurcation

For the diffusion system (1.1), we will consider the existence of Turing-Hopf bifurcation. The uniform steady state solution plays a key role. In [18], the authors found that system (1.1) has a unique uniform steady state solution $E^* = (u^*, v^*)$, where $u^* = a, v^* = \frac{ab}{f(a)}$. For the homogeneous Neumann boundary conditions, we define the following real-valued Sobolev space

$$X = \{(u, v)^T \in H^2[(0, \ell\pi)] \times H^2[(0, \ell\pi)] : \frac{\partial u}{\partial x} = \frac{\partial v}{\partial x} = 0 \ \ at \ \ x = 0, \ell\pi\}$$

where $H^2[(0, \ell\pi)]$ is the standard Sobolev space. For $U_1 = (u_1, v_1)^T, U_2 = (u_2, v_2)^T \in X$,

we define the inner product

$$[U_1, U_2] = \int_0^{\ell\pi} (u_1 u_2 + v_1 v_2) \mathrm{d}x,$$

then X is a Hilbert space.

The linearized system of system (1.1) at E^* has the form

$$U_t = \mathcal{L}U := D\triangle U + J(u^*, v^*)U \tag{2.1}$$

where $U = (u, v)^T$,

$$D = \begin{pmatrix} d_1 & 0 \\ 0 & d_2 \end{pmatrix} \quad \text{and} \quad J(u^*, v^*) = \begin{pmatrix} -1 - b + \frac{abf'(a)}{f(a)} & f(a) \\ b - \frac{abf'(a)}{f(a)} & -f(a) \end{pmatrix}. \tag{2.2}$$

The operator $\mathcal{L}$ is linear on X. By the standard spectrum analysis as in [6, Theorem 1], we know that if all the spectra of the linear operator $\mathcal{L}$ have negative real parts, then E^* is local asymptotically stable, and if some spectrum have nonnegative real parts, then E^* is unstable.

The spectra of $-\triangle$ on $H^2[(0, \pi)]$ with homogeneous Neumann boundary condition are $\{k^2\}_{k\in\mathbb{N}_0}$and the corresponding normalized eigenfunctions are $\{\frac{1}{\sqrt{\pi}}, \sqrt{\frac{2}{\pi}}\cos(kx)\}_{k\in\mathbb{N}}$, see [11] . Hence the eigenvalues of operator $(u, v)^T \to (-d_1\triangle u, -d_2\triangle v)^T$ on X are $\{\frac{d_1 k^2}{\ell}, \frac{d_2 k^2}{\ell}\}_{k\in\mathbb{N}_0}$, and the corresponding normalized eigenfunctions are

$$\phi_k^{(1)} = \begin{pmatrix} \gamma_k(x) \\ 0 \end{pmatrix} \quad \text{and} \quad \phi_k^{(2)} = \begin{pmatrix} 0 \\ \gamma_k(x) \end{pmatrix}, \quad k \in \mathbb{N}_0 \tag{2.3}$$

where $\gamma_0(x) = \frac{1}{\sqrt{\ell\pi}}, \gamma_k(x) = \sqrt{\frac{2}{\ell\pi}}\cos(\frac{k}{\ell}x), k \in \mathbb{N}$.

Since $\{\phi_k^{(1)}, \phi_k^{(2)}\}_{k\in\mathbb{N}_0}$ is a basis of X, then for any $(\phi, \varphi) \in X$, there is a unique decomposition $(\phi, \varphi)^T = \sum\limits_{k=0}^{\infty}(a_k\phi_k^{(1)}(x) + b_k\phi_k^{(2)}(x))$, where $a_k, b_k \in \mathbb{R}$ are coefficients. For the spectra of $\mathcal{L}$ in X, we consider the characteristic equation $\mathcal{L}(\phi, \varphi)^T = \lambda(\phi, \varphi)^T$ on X. By the formula of $\mathcal{L}$, we have

$$(J(u^*, v^*) - \frac{k^2}{\ell^2}D)\sum_{k=0}^{\infty}(a_k\phi_k^{(1)}(x) + b_k\phi_k^{(2)}(x)) = \lambda\sum_{k=0}^{\infty}(a_k\phi_k^{(1)}(x) + b_k\phi_k^{(2)}(x)).$$

Hence, $(J(u^*, v^*) - \frac{k^2}{\ell^2}D)(a_k, b_k)^T = \lambda(a_k, b_k)^T,\ k \in \mathbb{N}_0$, where

$$J(u^*, v^*) - \frac{k^2}{\ell^2}D = \begin{pmatrix} -1 - b + \frac{abf'(a)}{f(a)} - \frac{k^2 d_1}{\ell^2} & f(a) \\ b - \frac{abf'(a)}{f(a)} & -f(a) - \frac{k^2 d_2}{\ell^2} \end{pmatrix}.$$

This means the spectra of the operator $\mathcal{L}$ are given by the eigenvalues of matrix $(J(u^*,v^*)-\frac{k^2}{\ell^2}D)$ for $k\in\mathbb{N}_0$, i.e.

$$\begin{aligned} F_k(\lambda) &= \left|\lambda E-(J(u^*,v^*)-\frac{k^2}{\ell^2}D)\right| \\ &= \lambda^2-T_k\lambda+D_k=0, \qquad k\in\mathbb{N}_0, \end{aligned} \tag{2.4}$$

where

$$\begin{aligned} T_k &= -1-f(a)-b[1-\frac{af'(a)}{f(a)}]-(d_1+d_2)\frac{k^2}{\ell^2}, \\ D_k &= f(a)+d_1d_2\frac{k^4}{\ell^4}+[d_1f(a)-d_2(\frac{abf'(a)}{f(a)}-b-1)]\frac{k^2}{\ell^2}. \end{aligned}$$

Recall that the bifurcation is called *Turing-Hopf bifurcation* if there exist a nonnegative integer k_1 and a positive integer $k_2\neq k_1$ such that $F_{k_1}(\lambda)=0$ has a pair of purely imaginary roots and $F_{k_2}(\lambda)=0$ has a simple zero root, and no other roots of the characteristic equation (2.4) have zero real parts, and the transversality condition holds.

First, we consider a special case. When $d_1=d_2=0$, there is no diffusion. From (2.4), we see that

$$T_0=-1-f(a)-b(1-\frac{af'(a)}{f(a)})=(b_h(a)-b)\frac{f(a)-af'(a)}{f(a)}, \quad D_0=f(a)>0$$

where $b_h(a)=-\frac{f(a)(1+f(a))}{f(a)-af'(a)}$.

For the sake of completeness, we give the following lemma on the stability of the positive equilibrium E^* with $d_1=d_2=0$.

Lemma 2.1. *Assume that the system* (1.1) *with* $d_1=d_2=0$, *then we have that*
(1) if $f(a)\geq af'(a)$ *or* $f(a)<af'(a)$ *and* $b<b_h(a)$, *then* E^* *is local asymptotically stable;*
(2) if $f(a)<af'(a)$ *and* $b=b_h(a)$, *then the Hopf bifurcation occurred near the* E^**;*
(3) if $f(a)<af'(a)$ *and* $b>b_h(a)$, *then* E^* *is unstable.*

Then we study the dynamics of the full reaction-diffusion system ($d_1,d_2>0$). We introduce some notations as $d_2>d_1$. Let $l(x)=\frac{d_1d_2x^2}{(d_2-d_1)x-1}, k_1^*=\lceil\frac{\ell}{\sqrt{d_2-d_1}}\rceil$ and $k_2^*=\max\{k_1^*+1,\lceil\frac{\sqrt{2}\ell}{\sqrt{d_2-d_1}}\rceil\}$, where $\lceil\cdot\rceil$ denotes the integral function defined in $\mathbb{N}_0$. Define

$$k^*=\begin{cases} k_2^*, & if \quad l(\frac{k_2^{*2}}{\ell^2})\leq l(\frac{(k_2^*+1)^2}{\ell^2}) \\ k_2^*+1, & if \quad l(\frac{k_2^{*2}}{\ell^2})>l(\frac{(k_2^*+1)^2}{\ell^2}) \end{cases}. \tag{2.5}$$

Set $\omega_c=\sqrt{l(\frac{k^{*2}}{\ell^2})}$ and $b(k,a)=\frac{d_1d_2\frac{k^4}{\ell^4}+[d_1f(a)+d_2]\frac{k^2}{\ell^2}+f(a)}{d_2(\frac{af'(a)}{f(a)}-1)\frac{k^2}{\ell^2}}$.

Theorem 2.1. *(1) Assume that $d_1 \geq d_2 > 0$, then we have following results:*

(i) if $f(a) \geq af'(a)$ or $f(a) < af'(a)$ and $b < b_h(a)$, then E^* is local asymptotically stable;

(ii) if $f(a) < af'(a)$ and $b > b_h(a)$, then E^* is unstable.

(2) Assume that $d_2 > d_1 > 0$, then we have following results:

(i) if $f(a) \geq af'(a)$ or $f(a) < af'(a), f(a) \leq l(\frac{k^{*2}}{\ell^2})$ and $b < b_h(a)$, then E^* is local asymptotically stable;

(ii) if $f(a) < af'(a)$ and $b > b_h(a)$, then E^* is unstable;

(iii) if $l(\frac{k^{*2}}{\ell^2}) < f(a) < af'(a)$ and $b(k^*, a) < b < b_h(a)$, then E^* is unstable and the Turing instability occurs;

(iv) if $f(a) = l(\frac{k^{*2}}{\ell^2}) < af'(a)$ and $b = b_h(a)$, then system (1.1) undergoes Turing-Hopf bifurcation in the vicinity of the E^*.

Proof. From the formulas of T_k and D_k of (2.4), one can see that when $f(a) \geq af'(a)$ or $f(a) < af'(a)$ and $b < b_h(a)$, then $T_k < 0$. Also, if $f(a) \geq af'(a)$, then $D_k > 0$ for $k \in \mathbb{N}_0$. In addition, when $d_1 \geq d_2 > 0$, we have

$$\begin{aligned} D_k &\geq f(a) + d_1 d_2 \frac{k^4}{\ell^4} + d_2[1 + f(a) - b(\frac{af'(a)}{f(a)} - 1)]\frac{k^2}{\ell^2} \\ &= f(a) + d_1 d_2 \frac{k^4}{\ell^4} + d_2(\frac{af'(a)}{f(a)} - 1)(b_h(a) - b)\frac{k^2}{\ell^2}, \end{aligned}$$

which implies that $D_k > 0$ for $k \in \mathbb{N}_0$ if $f(a) < af'(a)$ and $b < b_h(a)$. Hence $(1)(i)$ holds.

We consider the matrix $(J(u^*, v^*) - \frac{k^2}{\ell^2}D)$ for $k = 0$. When $f(a) < af'(a)$ and $b > b_h(a)$, we get that $T_0 > 0$ and $D_0 = f(a) > 0$. Hence the real parts of the eigenvalues of matrix $(J(u^*, v^*) - \frac{0}{\ell^2}D)$ are positive. Thus, the results of $(1)(ii), (2)(ii)$ hold.

For $d_2 > d_1 > 0$, $D_k > 0$ is equivalent to $b < b(k, a)$ for $k \in \mathbb{N}$. Note that

$$b(k, a) - b_h(a) = \frac{d_1 d_2 \frac{k^4}{\ell^4} + f(a)[1 - (d_2 - d_1)\frac{k^2}{\ell^2}]}{d_2(\frac{af'(a)}{f(a)} - 1)\frac{k^2}{\ell^2}}.$$

Then $b(k, a) > b_h(a)$ when $f(a) < af'(a)$ and $k \leq \frac{\ell}{\sqrt{d_2 - d_1}}$. This means that when $b < b_h(a)$ we have $D_k > 0$ for $k = 0, \cdots, k_1^*$. For $f(a) < af'(a)$ and $k \geq k_1^* + 1$, then $b(k, a) > b_h(a)$ if and only if $f(a) < l(\frac{k^2}{\ell^2})$. Note $l'(x) = \frac{d_1 d_2[(d_2 - d_1)x - 2]}{[(d_2 - d_1)x - 1]^2}$. Then $l(x)$ increases on $(0, \frac{2}{d_2 - d_1})$ and decreases on $(\frac{2}{d_2 - d_1}, \infty)$. Thus, $l(x)$ reaches its minimal value at $x = \frac{2}{d_2 - d_1}$. The equation (2.5) means that $l(\frac{k^2}{\ell^2})$ reaches its minimal value at $k = k^*$. Hence, when $f(a) < af'(a), k \geq k_1^* + 1$ and $f(a) \leq l(\frac{k^{*2}}{\ell^2})$, then $b(k, a) \geq b_h(a)$. Thence,

if $f(a) < af'(a), f(a) \le l(\frac{k^{*2}}{\ell^2})$ and $b < b_h(a)$, then $D_k > 0$ for $k \ge k_1^* + 1$. Hence, $(2)(i)$ is hold.

If $l(\frac{k^{*2}}{\ell^2}) < f(a) < af'(a)$, then $b(k^*, a) < b_h(a)$. When $d_2 > d_1 > 0$ and $b > b(k^*, a)$, we have $D_{k^*} < 0$. Thence, $(2)(iii)$ holds.

If $d_2 > d_1 > 0, f(a) = l(\frac{k^{*2}}{\ell^2}) < af'(a)$ and $b = b_h(a)$, then $T_0 = 0, T_k < 0$ for $k \in \mathbb{N}$ and $D_{k^*} = 0, D_k > 0$ for $k \in \mathbb{N}_0 \setminus \{k^*\}$. Also,

$$\frac{dT_0}{db}|_{b=b_h(a)} = \frac{af'(a)}{f(a)} - 1 > 0 \qquad and \qquad \frac{dD_{k^*}}{db}|_{b=b_h(a)} = -d_2\frac{k^2}{\ell^2}(\frac{af'(a)}{f(a)} - 1) < 0.$$

Therefore, $F_0(\lambda) = 0$ has a pair of purely imaginary roots $\lambda_{1,2} = \pm i\omega_c$, $F_{k^*}(\lambda) = 0$ has a simple zero root $\lambda_1 = 0$ and a negative real root $\lambda_2 = -(d_1 + d_2)\frac{k^{*2}}{\ell^2}$, and $F_k(\lambda) = 0$ has two negative real part roots for $k \in \mathbb{N}_0 \setminus \{0, k^*\}$. Then $(2)(iv)$ follows. □

3 Normal forms for Turing-Hopf bifurcation

From Theorem 2.1$(2)(iv)$, we know that, for fixed parameters ℓ, d_1, d_2, a^*, b^* such that $d_2 > d_1 > 0$, $f(a^*) = \frac{d_1 d_2 \frac{k^{*4}}{\ell^4}}{(d_2 - d_1)\frac{k^{*2}}{\ell^2} - 1} < a^* f'(a^*)$ and $b^* = b_h(a^*)$, where k^* is defined as in (2.5), then the equilibrium E^* is a Turing-Hopf bifurcation point of system (1.1). There may occur Hopf and saddle-node bifurcations near E^*. Then there is a local center manifold of codimension 3 in the phase space. We use the normal form on the center manifold to consider the spatiotemporal dynamics in a small neighbourhood of Turing-Hopf bifurcation point E^* of system (1.1). Choose a and b as the bifurcation parameters and set $a = a^* + \varepsilon_1, b = b^* + \varepsilon_2$. Then (1.1) becomes

$$\begin{cases} \frac{\partial u}{\partial t} = d_1 \triangle u + a^* + \varepsilon_1 - (1 + b^* + \varepsilon_2)u + f(u)v \\ \frac{\partial v}{\partial t} = d_2 \triangle v + (b^* + \varepsilon_2)u - f(u)v \end{cases}. \tag{3.1}$$

System (3.1) has a unique uniform steady state solution $E^* = (u^*(\varepsilon), v^*(\varepsilon))$, where $u^*(\varepsilon) = a^* + \varepsilon_1, v^*(\varepsilon) = \frac{(a^* + \varepsilon_1)(b^* + \varepsilon_2)}{f(a^* + \varepsilon_1)}$. Transfer $(u^*(\varepsilon), v^*(\varepsilon))$ to the origin by $u_1 = u - u^*(\varepsilon)$ and $v_1 = v - v^*(\varepsilon)$, then system (3.1) becomes

$$\frac{\partial U_1}{\partial t} = D \triangle U_1 + J(u^*(0), v^*(0))U_1 + g(U_1, \varepsilon), \tag{3.2}$$

where $U_1 = (u_1, v_1)^T, D$ and $J(u^*(0), v^*(0))$ be as in (2.2) and

$$g(U_1, \varepsilon) = \sum_{i+j+l_1+l_2 \ge 2}^{\infty} \frac{1}{i!j!l_1!l_2!} g_{ij}^{(l_1 l_2)} u_1^i v_1^j \varepsilon_1^{l_1} \varepsilon_2^{l_2} \begin{pmatrix} 1 \\ -1 \end{pmatrix} := \sum_{n \ge 2}^{\infty} \frac{1}{n!} g_n(U_1, \varepsilon), \tag{3.3}$$

with $g_{ij}^{(l_1l_2)} = \frac{\partial^{i+j+l_1+l_2}F(0,0,0,0)}{\partial u_1^i v_1^j \varepsilon_1^{l_1}\varepsilon_2^{l_2}}$ and $F(u_1, v_1, \varepsilon_1, \varepsilon_2) = -u_1\varepsilon_2 + f(u_1 + u^*(\varepsilon))(v_1 + v^*(\varepsilon))$. We list some coefficients which will be used in the sequel:

$$\begin{aligned}
g_{10}^{(10)} &= \frac{b^*f'(a^*)}{f(a^*)} + \frac{a^*b^*f''(a^*)}{f(a^*)} - \frac{a^*b^*f'^2(a^*)}{f^2(a^*)},\ g_{10}^{(01)} = \frac{a^*f'(a^*)}{f(a^*)} - 1,\\
g_{01}^{(01)} &= g_{02}^{(00)} = 0, g_{01}^{(10)} = g_{11}^{(00)} = f'(a^*), g_{(20)}^{(00)} = \frac{a^*b^*f''(a^*)}{f(a^*)},\\
g_{20}^{(10)} &= \frac{f''(a^*)b^*}{f(a^*)} + \frac{a^*b^*f'''(a^*)}{f(a^*)} - \frac{a^*b^*f'(a^*)f''(a^*)}{f^2(a^*)}, g_{12}^{(00)} = g_{03}^{(00)} = 0\\
g_{20}^{(01)} &= \frac{a^*f''(a^*)}{f(a^*)}, g_{11}^{(10)} = g_{21}^{(00)} = f''(a^*),\ g_{30}^{(00)} = \frac{a^*b^*f'''(a^*)}{f(a^*)}.
\end{aligned}$$

Consider the linear part of system (3.2) at the origin

$$\frac{\partial U_1}{\partial t} = \mathcal{L}(U_1) := D\triangle U_1 + J(u^*(0), v^*(0))U_1. \tag{3.4}$$

In fact, the set of all eigenvalues of system (3.4) with zero real part is $\Lambda = \{\pm\omega_c, 0\}$. Our strategy is to decompose X into the eigenvector spaces and consider (3.4) in each eigenvector space. From (2.3), we set $\zeta_k = span\{[\varphi, \phi_k^{(i)}]\phi_k^{(i)} | \varphi \in X, i = 1, 2\}$. Then $J(u^*(0), v^*(0))\zeta_k \subset span\{\phi_k^{(1)}, \phi_k^{(2)}\}, k \in \mathbb{N}_0$. Set $y(t) = (y_1(t), y_2(t)) \in \mathbb{R}^2$ such that $y_1\phi_k^{(1)} + y_2\phi_k^{(2)} \in \zeta_k$. When (3.4) is restricted on ζ_k, it is becomes the following ordinary differential equation on $\mathbb{R}^2$

$$\dot{y}(t) = \begin{bmatrix} \frac{a^*b^*f'(a^*)}{f(a^*)} - b^* - 1 - d_1\frac{k^2}{\ell^2} & f(a^*) \\ b^* - \frac{a^*b^*f'(a^*)}{f(a^*)} & -f(a^*) - d_2\frac{k^2}{\ell^2} \end{bmatrix} y(t) := J_k(u^*(0), v^*(0))y(t). \tag{3.5}$$

Restricted on ζ_k, we know that (3.4) and (3.5) have the same eigenvalues. Hence, Λ is the only eigenvalues of $J_k(u^*(0), v^*(0))$, which has eigenvalues with zero real part for some $k \in \mathbb{N}_0$.

Since (3.5) is invariant on ζ_k, we project X into the generalized eigenspaces of eigenvalues Λ. Generally, we decompose $\mathbb{C}^2$ by the generalized eigenspace of $J_k(u^*(0), v^*(0))$. By the standard adjoint theory for ordinary differential equations, we can decompose $\mathbb{C}^2$ as $\mathbb{C}^2 = P_k \bigoplus Q_k$, where P_k is the generalized eigenspace associated with the eigenvalues in Λ and $Q_k = \{\phi \in \mathbb{C}^2 : \langle\phi, \varphi\rangle = 0 \text{ for all } \varphi \in P_k^*\}$, where P_k^* is the dual space of P_k and $\langle, \rangle$ is the scalar product of two complex vectors. For dual bases Φ_k and Ψ_k of P_k and P_k^*, we have $\langle\Phi_k, \Psi_k\rangle = I_{\varsigma_k}$, where $\varsigma_k = \dim P_k$ and I_{ς_k} is an $\varsigma_k \times \varsigma_k$ identity matrix. Notice that $\dim P_0 = 2$ and $\dim P_{k^*} = 1$. That is the center subspaces has dimension 3.

Through straightforward calculations, we obtain $\Phi_0 = (p_0, \overline{p}_0)$, $\Psi_0 = col(q_0^T, \overline{q}_0^T)$, $\Phi_{k^*} = p_{k^*}$ and $\Psi_{k^*} = q_{k^*}^T$, where

$$p_0 = \begin{pmatrix} 1 \\ -1 + \frac{1}{\omega_c} i \end{pmatrix}, \quad q_0 = \begin{pmatrix} \frac{1}{2} - \frac{\omega_c}{2} i \\ -\frac{\omega_c}{2} i \end{pmatrix}, \quad p_{k^*} = \begin{pmatrix} 1 \\ \frac{d_1 k^{*2}}{\omega_c^2 \ell^2} - 1 \end{pmatrix}, \quad q_{k^*} = \begin{pmatrix} \frac{d_2}{d_1+d_2} - \frac{\omega_c^2}{T_{k^*}} \\ -\frac{\omega_c^2}{T_{k^*}} \end{pmatrix},$$

with $T_{k^*} = -\frac{k^{*2}}{\ell^2}(d_1 + d_2)$.

Then, by the procedure developed in [44, 45, 47], the normal form for Turing-Hopf bifurcation point E^* can be obtained as follows

$$\begin{cases} \dot{r} = \zeta_1(\varepsilon) r + \kappa_{11} r^3 + \kappa_{12} r \rho^2 \\ \dot{\rho} = \zeta_2(\varepsilon) \rho + \kappa_{21} r^2 \rho + \kappa_{22} \rho^3 \end{cases} \tag{3.6}$$

with $\zeta_1(\varepsilon) = \frac{Re(B_{11})}{2}\varepsilon_1 + \frac{B_{12}}{2}\varepsilon_2, \zeta_2(\varepsilon) = \frac{d_2}{d_1+d_2}(B_{31}\varepsilon_1 + B_{32}\varepsilon_2), \kappa_{11} = Re(B_{210}), \kappa_{12} = Re(B_{102}), \kappa_{21} = B_{111}, \kappa_{22} = B_{003}$, where $B_{11} = g_{10}^{(10)} - g_{01}^{(10)} + i\frac{g_{01}^{(10)}}{\sqrt{f(a^*)}}, B_{12} = g_{10}^{(01)}, B_{31} = g_{10}^{(10)} - g_{01}^{(10)} + \frac{d_1 k^{*2}}{f(a^*)\ell^2} g_{01}^{(10)}, B_{32} = g_{10}^{(01)}$, the calculation of $B_{210}, B_{102}, B_{111}$ and B_{003}, we leave them in Appendix.

By the center manifold theorem in [5] and the bifurcation theorem in [10, 25], we know that the dynamics of system (3.1) is topologically equivalent to system (3.6) in a sufficiently small neighborhood of $\varepsilon = 0$. System (3.1) undergoes a Turing-Hopf bifurcation. Hence the system can coexist two spatially inhomogeneous steady states, a spatially inhomogeneous steady state coexist with a homogeneous periodic solution, coexist two spatially inhomogeneous periodic solution or spatially inhomogeneous periodic solution coexist with a homogeneous periodic solution and so on. The rich dynamics of the normal form (3.6), see [14, 25].

4 Numerical simulations

In this section, simulations were performed with MATLAB to illustrate our results. We take $f(u) = u^2$ and fix $(\ell, d_1, d_2, a, b) = (3, 0.2, 0.8, 1.3522, 2.8286)$. Then (ℓ, d_1, d_2, a, b) satisfies the conditions of Theorem 2.1(2)(iv). System (1.1) has a positive constant equilibrium $E^* = (1.3522, 2.0918)$ with $k^* = 6$ which is a Turing-Hopf point. We consider the Turing-Hopf bifurcation near E^* of system (1.1). In section 3, we have investigated the normal form of system (3.6) near E^*. For $(\ell, d_1, d_2, a, b) = (3, 0.2, 0.8, 1.3522, 2.8286)$, the normal form of equation (3.6)

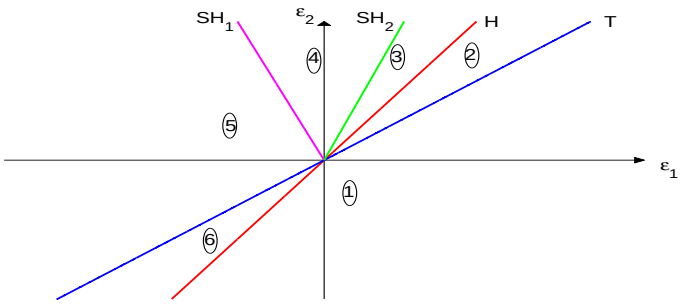

Figure 1: Bifurcation curve in $\varepsilon_1 - \varepsilon_2$ plane.

becomes

$$\begin{cases} \dot{r} = -(1.3522\varepsilon_1 - 0.5\varepsilon_2)r - 0.079r^3 - 0.0931r\rho^2 \\ \dot{\rho} = -(1.2169\varepsilon_1 - 0.8\varepsilon_2)\rho - 0.2793r^2\rho - 0.1214\rho^3 \end{cases}. \tag{4.1}$$

Notice that $r > 0$ and $\rho \in \mathbb{R}$. The equilibria of system (4.1) is as following: (4.1) has a zero equilibrium $E_0(0,0)$ for all $\varepsilon_1, \varepsilon_2$; three axis-equilibria $E_1(\sqrt{6.3291\varepsilon_2 - 17.1165\varepsilon_1}, 0)$ for $\varepsilon_2 > 2.7044\varepsilon_1$ and $E_2^{\pm}(0, \pm\sqrt{6.5898\varepsilon_2 - 10.0239\varepsilon_1})$ for $\varepsilon_2 > 1.5211\varepsilon_1$; and two interior equilibria $E_3^{\pm}(\sqrt{3.1014\varepsilon_1 + 0.8402\varepsilon_2}, \pm\sqrt{4.6616\varepsilon_2 - 17.1667\varepsilon_1})$ for $\varepsilon_2 > -3.6913\varepsilon_1$ and $\varepsilon_2 > 3.6826\varepsilon_1$.

In fact, the zero equilibrium E_0 of system (4.1) corresponds to the positive constant equilibrium E^* of the original system (1.1); the axis-equilibrium E_1 of system (4.1) corresponds to the spatially homogeneous periodic solution of the original system (1.1); the axis-equilibria $E_2^{\pm}$ of system (4.1) correspond to the nonconstant steady state solutions of the original system (1.1); and the interior equilibria $E_3^{\pm}$ of system (4.1) correspond to the spatially inhomogeneous periodic solutions of the original system (1.1), which has the spatial structure like $\cos 2x$ shape and periodic temporal structure since $\frac{k^*}{\ell} = 2$.

From the discussion above of existence conditions of equilibria, we have the following bifurcation lines

$$H:\ \varepsilon_2 = 2.7044\varepsilon_1; \qquad SH_1:\ \varepsilon_2 = -3.6913\varepsilon_1,\ \varepsilon_1 < 0;$$
$$T:\ \varepsilon_2 = 1.5211\varepsilon_1; \qquad SH_2:\ \varepsilon_2 = 3.6826\varepsilon_1,\ \varepsilon_1 > 0.$$

In the $\varepsilon_1 - \varepsilon_2$ parameter plane, these four lines divide a small neighborhood of the origin into six regions and the bifurcation diagram in the $\varepsilon_1 - \varepsilon_2$ parameter plane can be seen in Fig. 1. We discuss the dynamics in all the regions.

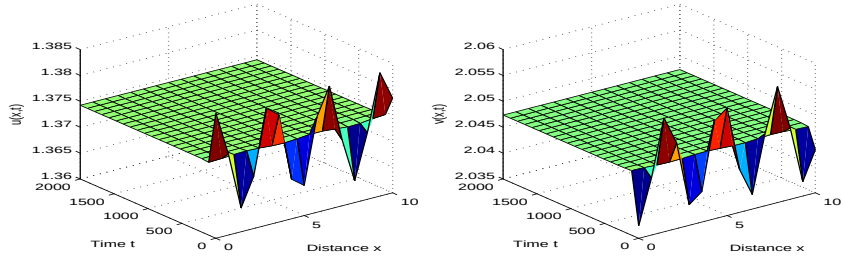

Figure 2: The positive constant equilibrium $E^*(1.3742, 2.0474)$ is asymptotically stable.

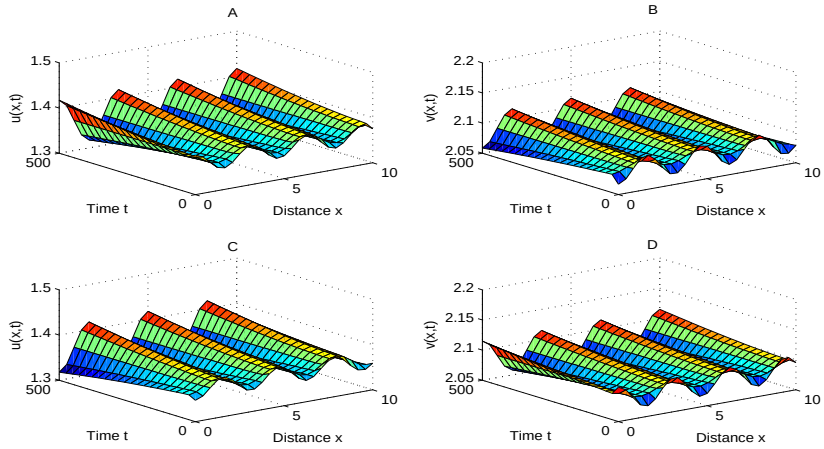

Figure 3: Two stable spatially inhomogeneous steady states like $\cos(2x)$.

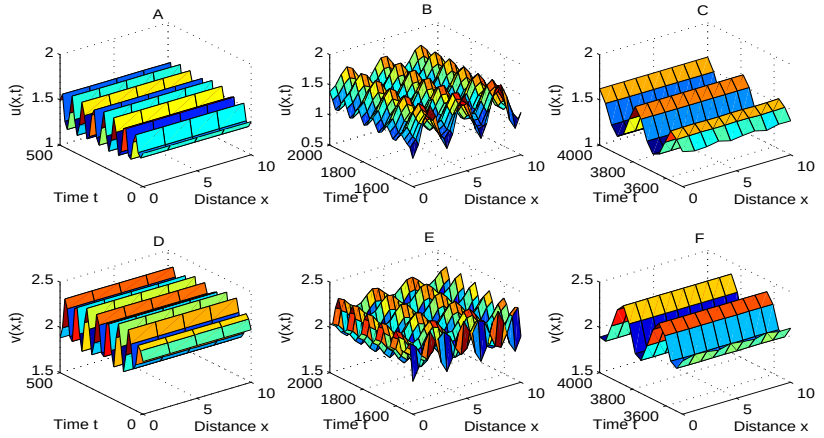

Figure 4: A heteroclinic orbit connecting the unstable spatially homogeneous periodic solution to stable spatially inhomogeneous steady state. A, D are transient behaviors for u and v, respectively; B, E are middle-term behaviours for u and v, respectively; C, F are long-term behaviors for u and v, respectively.

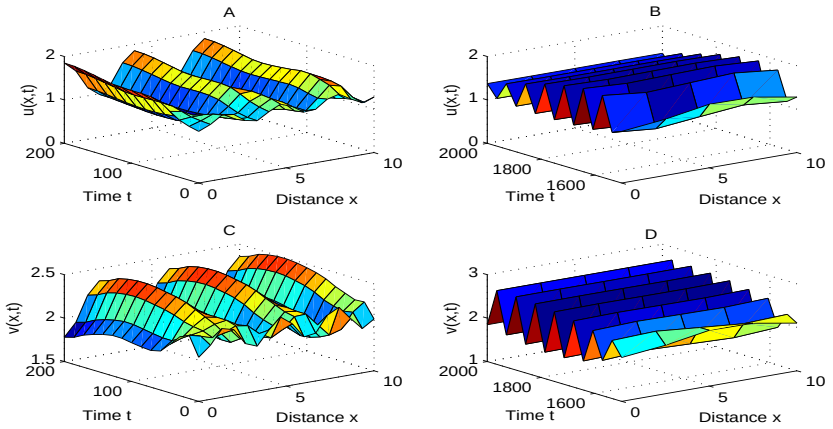

Figure 5: A heteroclinic orbit connecting the unstable spatially inhomogeneous periodic solution to stable spatially homogeneous periodic solution. A, C are transient behaviors for u and v, respectively; B, D are long-term behaviors for u and v, respectively.

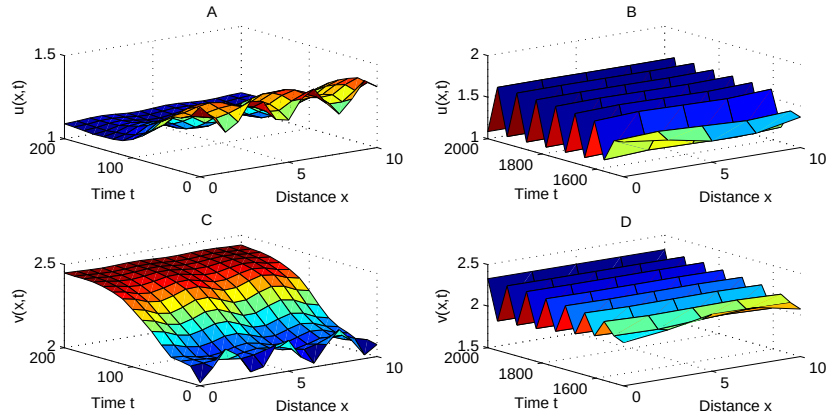

Figure 6: A heteroclinic orbit connecting the unstable spatially inhomogeneous steady state to stable spatially homogeneous periodic solution. A, C are transient behaviors for u and v, respectively; B, D are long-term behaviors for u and v, respectively.

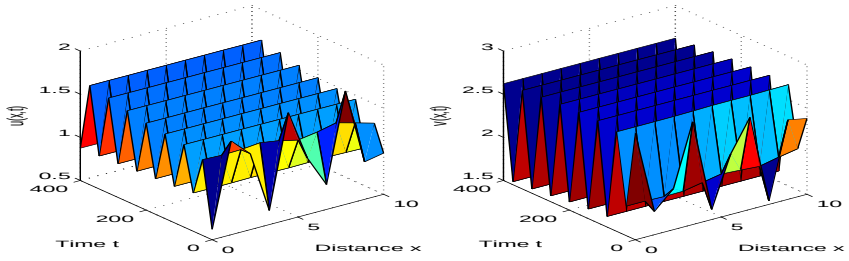

Figure 7: A stable spatially homogeneous periodic solution.

In region ①, system (4.1) has only one equilibrium E_0 and it is asymptotically stable. This implies that system (1.1) has a unique asymptotically stable positive constant equilibrium E^*. For $(\varepsilon_1, \varepsilon_2) = (0.021, -0.015)$ in region ①, which is shown in Fig. 2 for the initial condition $u(x,0) = 1.3742 + 0.01\cos(2x), v(x,0) = 2.0474 - 0.01\cos(2x)$.

In region ②, system (4.1) has three equilibria E_0, E_2^+ and E_2^-. Furthermore, E_0 is an unstable equilibrium and E_2^+, E_2^- are asymptotically stable equilibria. This implies that system (1.1) has an unstable positive constant equilibrium E^*, two stable spatially inhomogeneous steady states with inhomogeneous spatial structure like $\cos(2x)$ shape. For $(\varepsilon_1, \varepsilon_2) = (0.015, 0.025)$ in region ②, system (1.1) converge to one of these two nonconstant steady states with inhomogeneous spatial structure like $\cos(2x)$ shape, which are shown in Fig. 3 A, B for the initial condition $u(x,0) = 1.3672 + 0.02\cos(2x), v(x,0) = 2.0871 - 0.02\cos(2x)$ and Fig. 3 C, D for the initial condition $u(x,0) = 1.3672 - 0.02\cos(2x), v(x,0) = 2.0871 + 0.02\cos(2x)$.

In region ③, system (4.1) has four equilibria E_0, E_1, E_2^+ and E_2^-. And, E_0, E_1 are unstable equilibria and E_2^+, E_2^- are asymptotically stable equilibria. This means that system (1.1) has an unstable positive constant equilibrium E^*, an unstable spatially homogeneous periodic solution and two stable spatially inhomogeneous steady states with inhomogeneous spatial structure like $\cos(2x)$ shape. Take $(\varepsilon_1, \varepsilon_2) = (-0.012, -0.032)$ in region ③, the dynamics of system (1.1) evolves from an unstable homogeneous periodic solution to a stable spatially inhomogeneous steady state with inhomogeneous spatial structure like $\cos(2x)$ shape and there exists an orbit connecting the unstable spatially homogeneous periodic solution to the stable steady state, which is shown in Fig. 4 for the initial condition $u(x,0) = 1.3762 - 0.001\cos(2x), v(x,0) = 2.1104 - 0.001\cos(2x)$.

In region ④, system (4.1) has five equilibria $E_0, E_1, E_2^+, E_2^-, E_3^+$ and E_3^-. Moreover, E_0, E_3^+, E_3^- are unstable equilibria and E_1, E_2^+, E_2^- are asymptotically stable equilibrium. This means that system (1.1) has an unstable positive constant equilibrium E^*, two unstable spatially inhomogeneous periodic solutions with inhomogeneous spatial structure like $\cos(2x)$ shape and periodic temporal structure, a stable spatially homogeneous periodic solution and two stable spatially inhomogeneous steady states with inhomogeneous spatial structure like $\cos(2x)$ shape. Take $(\varepsilon_1, \varepsilon_2) = (-0.012, 0.063)$ in region ④, the dynamics of system (1.1) evolves from an unstable spatially inhomogeneous periodic solution with inhomogeneous spatial structure like $\cos(2x)$ shape and periodic temporal structure to stable spatially homogeneous periodic solu-

tion, which is shown in Fig. 5 for the initial condition $u(x,0) = 1.3342 - 0.15\cos(2x), v(x,0) = 2.1575 - 0.15\cos(2x)$.

In region ⑤, system (4.1) has four equilibria E_0, E_1, E_2^+ and E_2^-. And, E_0, E_2^+, E_2^- are unstable equilibria and E_1 is an asymptotically stable equilibrium. This means that system (1.1) has an unstable positive constant equilibrium E^*, two unstable steady states with inhomogeneous spatial structure like $\cos(2x)$ shape and a stable spatially homogeneous periodic solution. Take $(\varepsilon_1, \varepsilon_2) = (-0.023, -0.025)$ in region ⑤, the dynamics of system (1.1) evolves from an unstable spatially inhomogeneous steady state with inhomogeneous spatial structure like $\cos(2x)$ shape to stable spatially homogeneous periodic solution, which is shown in Fig. 6 for the initial condition $u(x,0) = 1.3292 + 0.09\cos(2x), v(x,0) = 2.1091 - 0.09\cos(2x)$.

In region ⑥, system (4.1) has two equilibria E_0 and E_1. And, E_0 is an unstable equilibrium and E_1 is an asymptotically stable equilibrium. This means that system (1.1) has an unstable positive constant equilibrium E^* and a stable spatially homogeneous periodic solution. Take $(\varepsilon_1, \varepsilon_2) = (0.023, 0.0635)$ in region ⑥, which is shown in Fig. 7 for the initial condition $u(x,0) = 1.2222 - 0.65\cos(2x), v(x,0) = 2.1342 + 0.65\cos(2x)$.

5 Conclusion

In this paper, we have studied the spatiotemporal dynamics of a reaction-diffusion system with general Brusselator type near the Turing-Hopf bifurcation point. By using the qualitative analysis, we prove the existence of the codimension-2 Turing-Hopf bifurcation and give out the precise conditions for the suitable ranges of the parameters. Then, by choose a, b as the bifurcation parameters, we derive the normal form for the Turing-Hopf bifurcation on the center manifold. And, according to the corresponding normal form, the complex spatiotemporal dynamics near the Turing-Hopf bifurcation point can be explicitly classified into six bifurcation scenarios, which are shown in Fig. 1. For each case, we have made some numerical simulations to illustrate our theoretical results.

In Ghergu et al. [18] and Li [30], the researchers mainly discussed the Turing instability or bifurcation analysis of codimension-1 such as Hopf bifurcation or steady state bifurcation. Combing the results in [18, 30] and our results in this paper, we see that the system has some interesting dynamics as the values of parameters of the model vary, such as the existence of an

unstable spatially homogeneous periodic solution and two stable spatially inhomogeneous steady states, the coexistence of two unstable spatially inhomogeneous periodic solutions.

6 Appendix: calculation of $B_{210}, B_{102}, B_{111}$ and B_{003}

$B_{210} = \frac{1}{4\ell\pi}(C_{210} - \frac{1}{2\omega_c}D_{210}), B_{102} = \frac{1}{4\ell\pi}(C_{102} - \frac{1}{2\omega_c}D_{102} + \frac{d_1}{d_1+d_2}E_{102}),$

$B_{111} = \frac{d_2}{\ell\pi(d_1+d_2)}(C_{111} - \frac{1}{\omega_c^2}D_{111} + \frac{d_1}{2(d_1+d_2)}E_{111}), B_{003} = \frac{d_2}{4\ell\pi(d_1+d_2)}(C_{003} - \frac{2}{\omega_c^2}D_{003} - E_{003}),$

where

$C_{210} = g_{30}^{(00)} + g_{21}^{(00)}(-3 + \frac{1}{\omega_c}i), C_{102} = g_{30}^{(00)} + g_{21}^{(00)}(\frac{2d_1k^{*2}}{\omega_c^2\ell^2} - 3 + \frac{1}{\omega_c}i),$

$C_{111} = g_{30}^{(00)} + g_{21}^{(00)}(\frac{d_1k^{*2}}{\omega_c^2\ell^2} - 3), C_{003} = g_{30}^{(00)} + 3g_{21}^{(00)}(\frac{d_1k^{*2}}{\omega_c^2\ell^2} - 1),$

$D_{210} = (2q_{110}^2 + \frac{1}{3}q_{020}^2 - q_{200}q_{110})i, D_{102} = (q_{110} - q_{200} + \frac{4d_2}{d_1+d_2}q_{101})q_{002}i,$

$D_{111} = q_{110}g_{11}^{(00)}, D_{003} = q_{002}g_{11}^{(00)}, E_{102} = \frac{q_{101}}{i\omega_c - T_{k^*}}(g_{20}^{(00)} - 2g_{11}^{(00)}),$

$E_{003} = \frac{q_{002}}{\frac{4d_1d_2k^{*4}}{\ell^4} - \omega_c^2}[-\frac{4d_2k^{*2}}{\ell^2}g_{20}^{(00)} + g_{11}^{(00)}(\frac{4d_1d_2k^{*4}}{\omega_c^2\ell^4} + 4T_{k^*} - 1)],$

$E_{111} = [-g_{20}^{(00)} + g_{11}^{(00)}(2 + \frac{d_2k^{*2}}{\omega_c^2\ell^2} - \frac{1}{\omega_c}i)]\frac{q_{011}}{i\omega_c + T_{k^*}} + [g_{20}^{(00)} - g_{11}^{(00)}(2 + \frac{d_2k^{*2}}{\omega_c^2\ell^2} + \frac{1}{\omega_c}i)]\frac{q_{101}}{i\omega_c - T_{k^*}},$

with

$q_{200} = \overline{q_{020}} = g_{20}^{(00)} - 2g_{11}^{(00)} + i\frac{2g_{11}^{(00)}}{\omega_c}, \ q_{002} = g_{20}^{(00)} - 2g_{11}^{(00)} + \frac{2d_1k^{*2}}{\omega_c^2\ell^2}g_{11}^{(00)},$

$q_{110} = g_{20}^{(00)} - 2g_{11}^{(00)}, \ q_{101} = \overline{q_{011}} = g_{20}^{(00)} + g_{11}^{(00)}(\frac{d_1k^{*2}}{\omega_c^2\ell^2} - 2 + i\frac{1}{\omega_c}).$

References

[1] J. F. G. Auchmuty, G. Nicolis, Bifurcation analysis of nonlinear reaction-diffusion equations - I: Evolution equations and the steady state solutions, *Bull. Math. Biol.* **37** (1975), 323−365.

[2] P. Ashwin, Z. Mei, Normal form for Hopf bifurcation of partial differential equations on the square, *Nonlinearity.* **8** (1995), 715−734.

[3] K. J. Brown, F. A. Davidson, Global bifurcation in the Brusselator system, *Nonlinear Anal.* **24** (1995), 1713−1725.

[4] M. Baurmann, T. Gross, U. Feudel, Instabilities in spatially extended predator-prey systems: spatio-temporal patterns in the neighborhood of Turing-Hopf bifurcations, *J. Theor. Biol.* **245** (2007), 220−229.

[5] J. Carr, Applications of Center Manifold Theory, *Springer-Verlag, New York*, 1981.

[6] R. G. Casten, C. J. Holland, Stability properties of solutions to systems of reaction-diffusion equations, *SIAM J. Appl. Math.* **33** (1977), 353−364.

[7] A. De Wit, D. Lima, et al. Spatiotemporal dynamics near a codimension-two point, *Phys. Rev. E.* **54** (1996), 261−271.

[8] J.C. Tzou, Y.P. Ma, et al, Homoclinic snaking near a codimension-two Turing-Hopf bifurcation point in the Brusselator model, *Phys. Rev. E.* **87** (2013):022098.

[9] T. K. Callahan, E. Knobloch, Pattern formation in three-dimensional reaction-diffusion systems, *Physica D.* **132** (1999), 339−362.

[10] S. N. Chow, J. K. Hale, Methods of Bifurcation Theory, *Springer-Verlag, New York*, 1982.

[11] R. Courant, D. Hilbert, Methods of mathematical physics, *Cambridge University Press*, 1953.

[12] T. Erneux, E. Reiss, Brusselator isolas, *SIAM J. Appl. Math.* **43** (1983), 1240−1246.

[13] G. H. Guo, J. H. Wu, X. H. Ren, Hopf bifurcation in general Brusselator system with diffusion, *Appl. Math. Mech. (English Ed.)* **32** (2011), 1177−1186.

[14] J. Guckenheimer, P. Holmes, Nonlinear Oscillations, Dynamical Systems, and Bifurcations of Vector Fields, *Springer-Verlag, New York*, 1983.

[15] M. Ghergu, Non-constant steady states for Brusselator type systems, *Nonlinearity* **21** (2008), 2331−2345.

[16] M. Ghergu, Steady-state solutions for Gierer-Meinhardt type systems with Dirichlet boundary condition, *Trans. Amer. Math. Soc.* **361** (2009), 3953−3976.

[17] M. Ghergu, V.Ră dulescu, A singular Gierer-Meinhardt system with different source terms, *Proc. Royal Soc. Edinburgh A.* **138** (2008), 1215−1234.

[18] M. Ghergu, V.Ră dulescu, Turing pattern in general reaction-diffusion system of Brusselator type, *Commun. Contemp. Math.* **12** (2010), 661−679.

[19] M. Ghergu, Steady-state solutions for a general Brusselator system, *Adv. Appl.* **216** (2011), 153−166.

[20] G. Iooss, M. Adelmeyer, Topics in bifurcation theory and applications, *Singapore, New Jersey, London: World Scientific Publishing Co.* 1992.

[21] M. Ipsen, F. Hynne, P. G. Sørensen, Amplitude equations for reaction-diffusion systems with a Hopf bifurcation and slow real modes, *Phys. D.* **13** (2000), 66−92.

[22] E. Karaoglu, H. Merdan, Hopf bifurcations of a ratio-dependent predator-prey model involving two discrete maturation time delays, *Chaos. Sol. Frac.* **68** (2014), 159−168.

[23] H. Kang, Dynamics of local map of a discrete Brusselator model: Eventually trapping regions and strange attractos, *Discrete Contin. Dyn. Syst.* **20** (2008), 939−959.

[24] P. D. Kepper, V. Castets, E. Dulos, J. Boissonade, Turing-type chemical patterns in the chlorite-iodide-malonic acid reaction, *Phys. D.* **49** (1991), 161−169.

[25] Y. A. Kuznetsov, Elements of Applied Bifurcation Theory, second ed., *Springer Verlag, New York*, 1998.

[26] B. Li, M. X. Wang, Diffusion-driven instability and Hopf bifurcation in Brusselator system, *Appl. Math. Mech. (English Ed.)* **29** (2008), 825-832.

[27] C. Li, H. Liu, T. Zhang, F. Yan, Network Mediated by Small Noncoding RNA with Time Delays and Diffusion, *Int. J. Bifurc. Chaos*, **27** (2017), 175−194.

[28] I. Lengyel, I. R. Epstein, A chemical approach to designing Turing patterns in reactiondiffusion system, *Proc. Natl. Acad. Sci. USA.* **89** (1992), 3977−3979.

[29] X. Liu,T. Zhang,X. Meng, T. Zhang, TuringCHopf bifurcations in a predatorCprey model with herd behavior, quadratic mortality and prey-taxis, *Physica A*, **496** (2018), 446−460.

[30] Y. Li, Hopf bifurcations in general systems of Brusselator type, *Nonlinear Anal: RWA.* **28** (2016), 32−47.

[31] M. Meixner, A. D. Wit, S. Bose, E. Scholl, Generic spatiotemporal dynamics near codimension-two Turing-Hopf bifurcations, *Phys. Rev. E.* **55** (1997), 6690−6697.

[32] Z. Mei, Numerical bifurcation analysis for reaction-diffusion equations, *Berlin:Springer Verlag*, 2000.

[33] G. Nicolis, Patterns of spatio-temporal organization in chemical and biochemical kinetics, *SIAM-AMS Proc.* **8** (1974), 33−58.

[34] I. Prigogine, R. Lefever, Symmetry breaking instabilities in dissipative systems II, *J. Chem. Phys.* **48** (1968), 1665−1700.

[35] R. Peng, M. X. Wang, Pattern formation in the Brusselator system, *J. Math. Anal. Appl.* **309** (2005), 151−166.

[36] R. Peng, M. X. Wang, On steady-state solutions of the Brusselator-type system, *Nonlinear Anal: Theo. Meth. Appl.* **71** (2009), 1389−1394.

[37] A. Rovinsky, M. Menzinger, Interaction of Turing and Hopf bifurcations in chemical systems, *Phys. Rev. A.* **46** (1998), 6315−6322.

[38] L. A. D. Rodrigues, D. C. Mistro, S. Petrovskii, Pattern formation, long-term transients, and the Turing-Hopf bifurcation in a space-and time-discrete predator-prey system, *Bull. Math. Biol.* **73** (2011), 1812−1840.

[39] P. Rabinowitz, Some global results for nonlinear eigenvalue problems, *J. Func. Anal.* **7** (1971), 487−513.

[40] S. G. Ruan, Diffusion-driven instability in the Gierer-Meinhardt model of morphogenesis, *Nat. Resour. Model.* **11** (1998), 131−142.

[41] E. E. Selkov, Self-oscillations in glycolysis, *Eur. J. Biochem.* **4** (1968), 79−86.

[42] J. Schnakenberg, Simple chemical reaction system with limit cycle behaviour, *J. Theor. Biol.* **81** (1979), 389−400.

[43] S. H. Strogatz, Nonlinear Dynamics and Chaos, *Westview Press*, 1994.

[44] Y. Song, X. Zou, Spatiotemporal dynamics in a diffusive ratio-dependent predator-prey model near a Hopf-Turing bifurcation point, *Comput. Math. Appl.* **67** (2014), 1978−1997.

[45] Y. Song, T. Zhang, Y. Peng, Turing-Hopf bifurcation in the reaction-diffusion equations and its applications, *Commun. Nonlinear Sci. Numer. Simul.* **33** (2016), 229−258.

[46] A. M. Turing, The chemical basis of morphogenesis, *Philos. Trans. A Ser. B.* **237** (1952), 37−72.

[47] X. Tang, Y. Song, Cross-diffusion induced spatiotemporal patterns in a predator-prey model with herd behavior, *Nonlinear Anal. RWA.* **24** (2015) 36−49.

[48] F. Q. Yi, J. J. Wei, J. P. Shi, Diffusion-driven instability and bifurcation in the Lengyel-Epstein system, *Nonlinear Anal: RWA.* **9** (2008), 1038−1051.

[49] Y. You, Global dynamics of the Brusselator equations, *Dyn. Partial Diff. Eqns.* **4** (2007), 167−196.

[50] T. Zhang, X.Liu, X. Meng, T. Zhang, Spatio-temporal dynamics near the steady state of a planktonic system,*Comput. Math. Appl.* **75** (2018), 4490−4504.